Research Article

Vibrational Spectroscopic Study of the Cocrystal Products Formed by Cinchona Alkaloids with 5-Nitrobarbituric Acid

Harry G. Brittain

Center for Pharmaceutical Physics, 10 Charles Road, Milford, NJ 08848, USA

Correspondence should be addressed to Harry G. Brittain; hbrittain@centerpharmphysics.com

X-ray powder diffraction, differential scanning calorimetry, infrared absorption spectroscopy, and Raman spectroscopy have been used to study the phenomenon of cocrystal formation in the molecular complexes formed by 5-nitrobarbituric acid with four cinchona alkaloids. The cocrystal products were found to contain varying degrees of hydration, ranging from no hydration in the nitrobarbiturate-quinidine cocrystal up to a 4.5-hydrate species in the nitrobarbiturate-cinchonine cocrystal. For the nitrobarbiturate cocrystals with cinchonine, cinchonidine, and quinidine, the predominant interaction was with the quinoline ring system of the alkaloid. However, for quinine, the predominant interaction was with the quinuclidine group of the alkaloid. These properties serve to demonstrate the utility of 5-nitrobarbituric acid as a preferred reagent for chemical microscopy, since the differing range of hydrate and structural types would serve to easily differentiate the cinchona alkaloids from each other, even when different compounds contained the same absolute configurations at their dissymmetric centers.

1. Introduction

The realization that cocrystallization of drug substances with other compounds could lead to modification of physical properties has led to a vitalization of the crystal engineering community and to substantial interest in the part of the pharmaceutical industry [1–5]. Aakeröy and Salmon have summarized a useful framework to describe cocrystal formation, where such crystalline solids result from the assembly of supramolecular synthons constructed from discrete neutral compounds (that are solids at ambient temperatures) and where the cocrystal is a structurally homogeneous crystalline material that contains these synthons in definite stoichiometric amounts [6].

However, the subject area of cocrystals extends much further back in time than the recent activity [7], with the properties of mixed systems being reported under the scope of a variety of definitions. Herbstein has categorized these as molecular compounds with localized or delocalized interactions and has provided an extensive review of donor-acceptor complexes, hydrogen-bonded molecular complexes, and π-molecular complexes [8]. Annual reviews summarizing advances in crystal engineering are available [9–11].

Another source of unrecognized cocrystals is contained within the extensive scope of analytical chemistry conducted under the general category of chemical microscopy, where analysts would prepare derivatives or adducts of an analyte species and then identify the analyte on the basis of the morphology of the crystalline products [12, 13]. For example, Clarke developed sensitive microchemical tests for the determination of anesthetics [14], antihistamines [15], antimalarials [16], and analgesics [17], while Chatten and coworkers developed chemical microscopic methods for the identification and differentiation of local anesthetics [18], muscle relaxants [19], and amine-containing compounds [20].

One of the premier chemical microscopic reagents was 5-nitrobarbituric acid (also known as dilituric acid), whose adduct complexes with basic compounds were superior to surpass other nitroenolic reagents owing to the high degree of crystallinity and ease of recrystallization of the products of [21]. Plein and Dewy developed the use of this compound as a reagent for the identification of aliphatic amines [22], primary aromatic amines [23], autonomic drugs [24], and secondary aromatic amines [25]. More recently, the underlying crystallographic properties associated with

adducts of 5-nitrobarbituric acid and basic compounds that facilitated their utility in chemical microscopy have been evaluated through the study of the cocrystals formed by the diliturate reagent with primary achiral phenylalkylamines [26] and resolved and racemic phenylalkylamines and phenylalkylamino acids [27]. In these works, it was established that the different crystal morphologies associated with the various reaction products were derived from the ability of the systems to form a variety of polymorphic and solvatomorphic cocrystal structures.

In the present work, the phenomenon of cocrystal formation in the molecular complexes of 5-nitrobarbituric acid has been further investigated through studies of adducts formed by this reagent with four cinchona alkaloids (quinine, quinidine, cinchonine, and cinchonidine). Structures of the 5-nitrobarbituric acid reagent and the alkaloids studies in this work are found in Figure 1. Although chemical microscopic identification methods have been published for cinchona alkaloids [28–30], the only report on the 5-nitrobarbiturate adducts simply mentioned the crystal morphologies of the quinine and cinchonine adducts [21]. Since no detailed studies of the cinchona alkaloid cocrystals with 5-nitrobarbituric acid have been reported, the products were characterized by the standard thermoanalytical and powder diffraction methods. In addition, detailed vibrational spectroscopic studies were performed in order to determine which vibrational modes were most affected by the cocrystal formation and to determine the magnitudes of perturbation within the involved vibrational modes.

2. Materials and Methods

2.1. Reagents and Method of Cocrystal Preparation. 5-Nitrobarbituric acid trihydrate, quinine dihydrate, quinidine, cinchonine, and cinchonidine were purchased from Sigma-Aldrich and were recrystallized from 70% aqueous isopropanol before use. The products studied in this work were prepared using solvent-drop-mediated solid-state grinding [31–33], where the stoichiometry of the product was determined by the amounts of reactants initially taken. Exactly weighed amounts of 5-nitrobarbituric acid and alkaloid acid were weighed directly in an agate mortar (preparing approximately 500 mg of total product) and wetted with 50 μL of 70% aqueous isopropanol. After slurry was prepared by mixing, the composition was hand-ground with an agate pestle until the product was completely dry.

2.2. X-Ray Powder Diffraction. X-ray powder diffraction (XRPD) patterns were obtained using a Rigaku MiniFlex powder diffraction system, equipped with a horizontal goniometer operating in the $\theta/2\theta$ mode. The X-ray source was nickel-filtered Kα emission of copper (1.54184 Å). Samples were packed into the sample holder using a back-fill procedure and were scanned over the range of 3.5 to 40 degrees 2θ at a scan rate of 0.5 degrees 2θ/min. Using a data acquisition rate of 1 point per second, the scanning parameters equate to a step size of 0.0084 degrees 2θ. Calibration of the diffractometer system was effected using purified talc as a reference material.

2.3. Thermal Analysis. Measurements of differential scanning calorimetry (DSC) were obtained on a TA Instruments 2910 thermal analysis system. Samples of approximately 1-2 mg were accurately weighed into an aluminum DSC pan and then covered with an aluminum lid that was crimped in place. The samples were then heated over the range of 20–175°C, at a heating rate of 10°C/min.

Measurements of total volatile content were made using an Ohaus model MB45 system. The samples were heated isothermally at a temperature of 125°C for a period of 15 minutes. Invariably, samples had desolvated to constant weight after approximately 10 minutes of heating time.

2.4. Infrared Absorption Spectroscopy. Infrared absorption spectra were obtained at a resolution of 4 cm^{-1} using a Shimadzu model 8400S Fourier-transform infrared spectrometer, with each spectrum being obtained as the average of 25 individual spectra. The data were acquired using the attenuated total reflectance sampling mode, where the samples were clamped against the ZnSe crystal of a Pike MIRacle single reflection horizontal ATR sampling accessory.

2.5. Raman Spectroscopy. Raman spectra were obtained in the fingerprint region using a Raman Systems model R-3000HR spectrometer, operated at a resolution of 5 cm^{-1} and using a laser wavelength of 785 nm. The data were acquired using front-face scattering from a thick powder bed kept in an aluminum sample holder.

3. Results and Discussion

3.1. Stereochemistry of the Cinchona Alkaloids. Examination of Figure 1 reveals the structural similarity of the cinchona alkaloids studied in the present work. The configurations of the compounds were once a matter of dispute, but a detailed study of the oxirane derivatives served to establish that all of the naturally occurring cinchona alkaloids are of the erythroconfiguration [34]. The members of this series each contain a quinoline ring attached through a hydroxymethylene group to a quinuclidine ring. As illustrated in the figure, cinchonine and cinchonidine represent a diastereomeric pair, but the important diastereomeric phenomena related to these compounds have been correlated with the absolute configuration at carbon-9 [35]. A more systematic name for cinchonine is (9*S*)-cinchonan-9-ol, and the more systematic name for cinchonidine is (9*R*)-cinchonan-9-ol. The absolute configurations of all centers of dissymmetry are known [36].

Quinine and quinidine are also a diastereomeric pair and differ from cinchonine and cinchonidine by the presence of a methoxy group attached to the quinoline ring. The more systematic name for quinidine is (9*S*)-6′-methyoxycinchonan-9-ol, while the more systematic name for quinine is (9*R*)-6′-methyoxycinchonan-9-ol. The absolute configuration of quinidine has been confirmed from a single-crystal study of one of its salts, with the absolute stereochemistry being determined by the Bijvoet anomalous-dispersion method [37]. As indicated in Figure 1, the dissymmetric centers of cinchonine
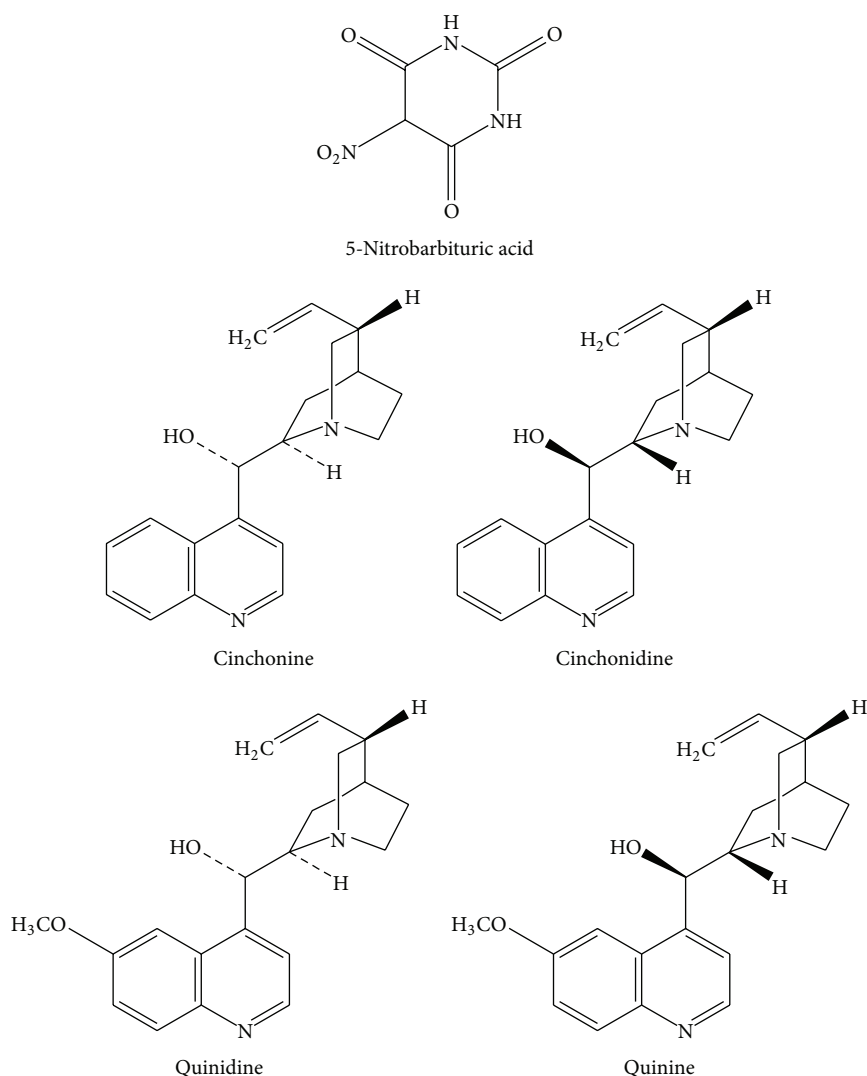
FIGURE 1: Structures of 5-nitrobarbituric acid and the four cinchona alkaloids used in this study.

and quinidine are the same, while the dissymmetric centers of cinchonidine and quinine are the same.

3.2. Vibrational Spectroscopy of 5-Nitrobarbituric Acid. Although the vibrational spectra of a large number of substituted barbituric acids have been reported and analyzed [38], the infrared absorption and Raman spectra of the 5-nitro derivative seem to have escaped attention. Fortunately, when one takes into account the inductive effect of the 5-nitro group on the assignments previously published for the energies of the vibrational modes of other barbiturate derivatives [39–42] and with the body of group frequency knowledge [43–50], one may deduce assignments for the absorption bands that will be important in the discussions. It may be noted that the broad but intense character of associated with the high-frequency vibrational modes (i.e., 2500–$3800 \, cm^{-1}$) greatly weakened the utility of this spectral region for evaluation of intermolecular interactions.

It is known that the vibrational motions of the three carbonyl groups on the barbituric acid moiety are observed as transitions into three-group frequency ring modes, and the atomic numbering shown in Figure 2 will be useful.

The highest frequency band (observed at an energy of $1705 \, cm^{-1}$ in the infrared absorption spectrum of 5-nitrobarbituric acid) is identified as the 4,6-CO symmetric mode, where the vibrational motion is more localized on the carbonyl groups located at carbons 4 and 6. The lowest frequency mode corresponds to the 2-CO stretching mode and is observed at an energy of $1614 \, cm^{-1}$, while the 4,6-CO antisymmetric mode is observed at an intermediate energy of $1651 \, cm^{-1}$. Other important absorption bands in the infrared absorption spectrum of 5-nitrobarbituric acid are the symmetric stretching mode associated with the nitro group ($1381 \, cm^{-1}$), the C–N ring deformation mode ($1246 \, cm^{-1}$), and the carbonyl out-of-plane bending mode ($779 \, cm^{-1}$).

A number of important bands were observed in the Raman spectrum of 5-nitrobarbituric acid, with these being
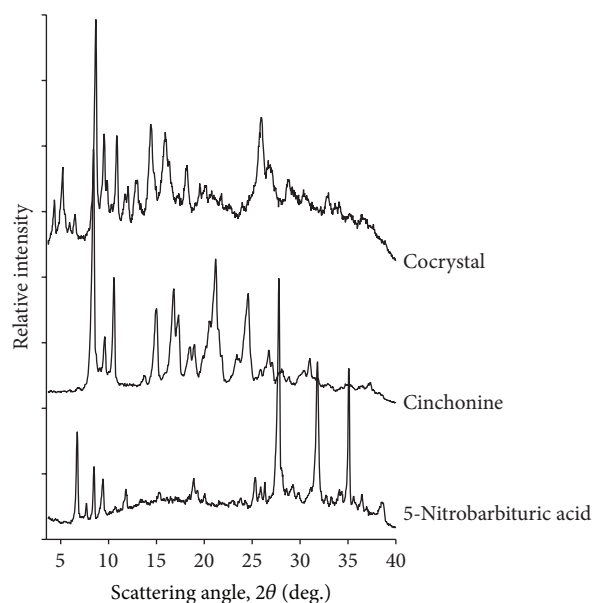
Figure 2

Figure 3: X-ray powder diffraction patterns of 5-nitrobarbituric acid, cinchonine, and the 1:1 nitrobarbituric-cinchonine cocrystal.

primarily associated with motions of the carbonyl groups. An in-plane bending mode was observed at an energy of $379 \, cm^{-1}$, while out-of-plane bending modes were observed at 625 and $695 \, cm^{-1}$. Other band assignments that will be important to succeeding discussion are an N–H out-of-plane bending mode ($846 \, cm^{-1}$), a C–N stretching mode ($1150 \, cm^{-1}$), and a C–N deformation mode ($1255 \, cm^{-1}$).

3.3. Vibrational Spectroscopy of the Cinchona Alkaloids.
While the vibrational modes of 5-nitrobarbituric acid are dominated by ring character, the vibrational modes of the cinchona alkaloids consist mainly of ring modes associated with the quinoline ring and C–C and C–H vibrational modes associated with the vinylquinuclidine group and the aliphatic linkage between the two. Since the vibrational spectroscopy of both quinoline [51, 52] and quinuclidine [53, 54] is well understood, the major transitions observed in the infrared absorption spectra and the Raman spectra of the cinchona alkaloids can be understood, especially when one considers studies that have been conducted on cinchonine [55], cinchonidine [56], and quinine [57]. Owing to the delocalized nature of the vibrational modes in these molecules, it is difficult to separate out individual modes that are localized on one of the important functional groups. However, the consensus opinion is that a nonprotonated quinuclidine will exhibit a vibrational mode in the range of approximately $1355–1365 \, cm^{-1}$ that shifts to a range of approximately $1380–1390 \, cm^{-1}$ upon protonation. A nonprotonated quinoline will exhibit a characteristic transition in the range of approximately $1570–1580 \, cm^{-1}$ which will shift to approximately $1600–1610 \, cm^{-1}$ upon protonation.

Unfortunately, were the protonated cinchona bands to be present in the absorption spectrum of a cocrystal product, they would be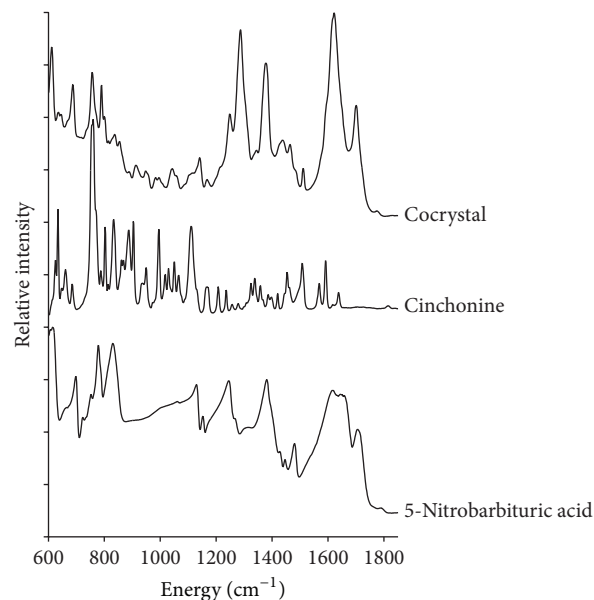 overwhelmed by the more intense absorption bands associated with the 5-nitrobarbituric acid. Fortunately, the Raman spectrum of the cinchona alkaloids is not so compromised, and one may readily assess the interactions existing in the cocrystal by tracking the energies of the key quinoline and quinuclidine vibrational modes.

3.4. The 1:1 Cinchonine Cocrystal Formed with 5-Nitrobarbituric Acid.
XRPD patterns obtained for 5-nitrobarbituric acid, cinchonine, and the nitrobarbiturate-cinchonine cocrystal product are shown in Figure 3. The differences between the diffraction patterns demonstrated that the three crystal structures are different and established the formation of a crystalline cocrystal product.

The nitrobarbiturate-cinchonine cocrystal product was found to evolve 14.8% of its mass when heated isothermally at 125°C, which would correspond to the existence of a 4.5-hydrate form of the cocrystal. The DSC thermogram of the cocrystal product consisted of a strong desolvation endothermic transition, characterized by a temperature maximum of 80°C and an enthalpy of fusion equal to 246 J/g. The desolvated compound formed upon completion of this thermal reaction did not exhibit a melting endothermic transition, indicating that an amorphous substance formed upon desolvation. The only other thermally induced transition observed in the DSC thermogram was the onset of decomposition, which began at a temperature of approximately 220°C.

The infrared absorption spectra obtained for 5-nitrobarbituric acid, cinchonine, and the 1:1 nitrobarbituric-cinchonine cocrystal within the fingerprint region are shown in Figure 4, and the correlation between the energies of the important absorption bands is shown in Table 1. All of the strong 5-nitrobarbiturate absorption bands were visible in the spectrum of the cocrystal, and most of these were found to be considerably shifted in energy relative to the free acid.

TABLE 1: Assignments of the major bands in the fingerprint region of the infrared absorption spectra of 5-nitrobarbituric acid, cinchonine, and their 1:1 cocrystal product.

| Assignment	Nitrobarbituric (cm^{-1})	Cocrystal (cm^{-1})	Cinchonine (cm^{-1})	Assignment
Carbonyl out-of-plane bending mode	779	756		
C–N ring deformation mode	1246	1286		
		Obscured and not observed	1360	Nonprotonated quinuclidine mode
Nitro group symmetric stretching mode	1381	1377		
		Obscured and not observed	1566	Nonprotonated quinoline mode
2-CO stretching mode	1614	1622		
4,6-CO antisymmetric mode	1651	Not observed		
4,6-CO symmetric mode	1705	1701		
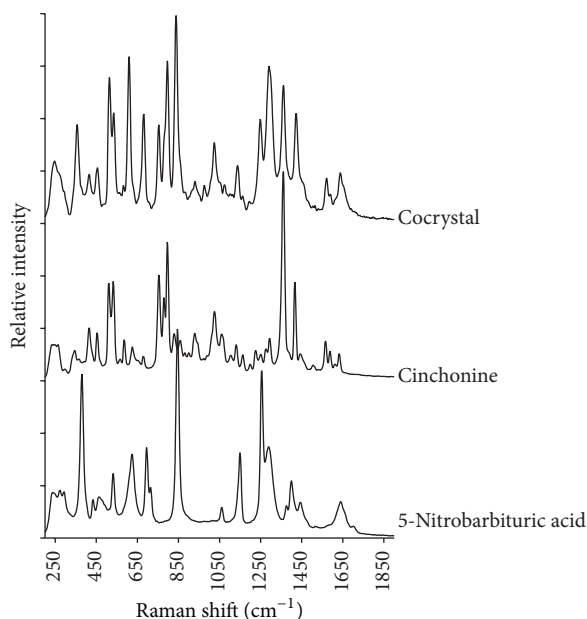
FIGURE 4: Infrared absorption spectra within the fingerprint region of 5-nitrobarbituric acid, cinchonine, and the 1:1 nitrobarbituric-cinchonine cocrystal.

FIGURE 5: Raman spectra within the fingerprint region of 5-nitrobarbituric acid, cinchonine, and the 1:1 nitrobarbituric-cinchonine cocrystal.

This finding demonstrates that the entire ring system of the acid is involved in the cocrystal formation. Unfortunately, the two key absorption bands of the quinuclidine and quinoline moieties of cinchonine were obscured by the nitrobarbiturate absorption bands and thus could not be used in an interpretative analysis.

The Raman spectra obtained for 5-nitrobarbituric acid, cinchonine, and the 1:1 nitrobarbituric-cinchonine cocrystal within the fingerprint region are shown in Figure 5, and the correlation between the energies of the important absorption bands is shown in Table 2. Once again, all of the strong 5-nitrobarbiturate vibrational modes were noted to undergo shifts in energy relative to the free acid, providing a further demonstration that the entire ring system of the acid is
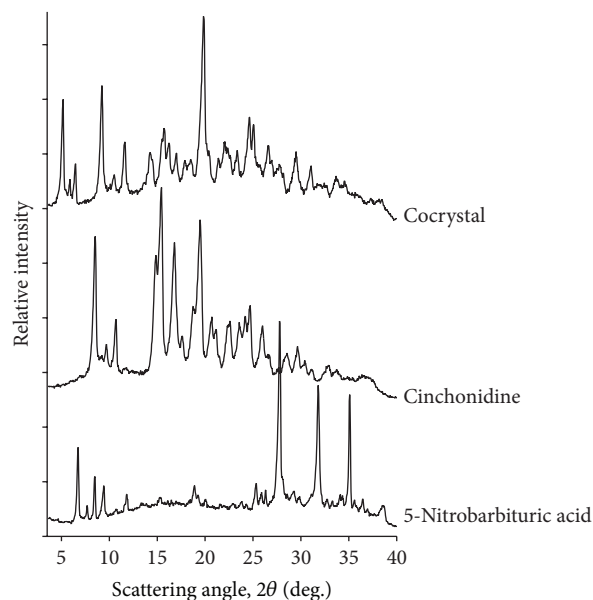
involved in the cocrystal formation. More importantly, the key Raman bands associated with cinchonine were visible in the spectrum of the cocrystal. The energy of the quinuclidine mode was not found to shift in the spectrum of the cocrystal, indicating that the degree of interaction with 5-nitrobarbituric acid at the tertiary nitrogen was minimal. The vibrational mode of the quinoline moiety did undergo a significant increase in energy, indicating that the predominant interaction with the acid took place at this group.

3.5. The 1:1 Cinchonidine Cocrystal Formed with 5-Nitrobarbituric Acid. The XRPD patterns obtained for 5-nitrobarbituric acid, cinchonidine, and the nitrobarbiturate-cinchonidine cocrystal product are shown in Figure 6. The fact that the powder pattern of the 1:1 stoichiometric reaction product

TABLE 2: Assignments of the major bands in the fingerprint region of the Raman spectra of 5-nitrobarbituric acid, cinchonine, and their 1:1 cocrystal product.

Assignment	Nitrobarbituric (cm^{-1})	Cocrystal (cm^{-1})	Cinchonine (cm^{-1})	Assignment
Carbonyl in-plane bending mode	379	357		
Carbonyl out-of-plane bending mode	625	609		
Carbonyl out-of-plane bending mode	695	681		
N–H out-of-plane bending mode	846	838		
C–N stretching mode	1150	1137		
C–N deformation mode	1255	1248		
		1361	1360	Nonprotonated quinuclidine mode
		1572	1566	Nonprotonated quinoline mode

TABLE 3: Assignments of the major bands in the fingerprint region of the infrared absorption spectra of 5-nitrobarbituric acid, cinchonidine, and their 1:1 cocrystal product.

Assignment	Nitrobarbituric (cm^{-1})	Cocrystal (cm^{-1})	Cinchonidine (cm^{-1})	Assignment
Carbonyl out-of-plane bending mode	779	762		
C–N ring deformation mode	1246	1256		
		Obscured and not observed	1352	Nonprotonated quinuclidine mode
Nitro group symmetric stretching mode	1381	1358		
		Obscured and not observed	1568	Nonprotonated quinoline mode
2-CO stretching mode	1614	1595		
4,6-CO antisymmetric mode	1651	1666		
4,6-CO symmetric mode	1705	1691		

cannot be obtained by a simple averaging of the XRPD patterns of the two reactants establishes the formation of a crystalline cocrystal product.

The nitrobarbiturate-cinchonidine cocrystal product was found to evolve 5.5% of its mass when heated isothermally at 125°C, which would correspond to the existence of a 1.5-hydrate form of the cocrystal. The DSC thermogram of the cocrystal product consisted of a strong desolvation endothermic transition, characterized by a temperature maximum of 101°C and an enthalpy of fusion equal to 97 J/g. The desolvated compound formed upon completion of this thermal reaction was found to exhibit a melting endothermic transition having a temperature maximum of 219°C, but as this transition was coupled with an exothermic decomposition reaction no estimation of enthalpy could be made.

The fingerprint region infrared absorption spectra obtained for 5-nitrobarbituric acid, cinchonidine, and the cocrystal product are shown in Figure 7, and the correlation between the energies of the important absorption bands is shown in Table 3. As had been noted for the 5-nitrobarbituric acid cocrystal with cinchonine, all of the strong nitrobarbiturate absorption bands in the spectrum of the cocrystal were found to be shifted in energy relative to the free acid. As before, the two key absorption bands of the quinuclidine and quinoline moieties of cinchonidine were obscured by the nitrobarbiturate absorption bands and were not available for analysis.

The fingerprint region Raman spectra obtained for 5-nitrobarbituric acid, cinchonidine, and the 1:1 nitrobarbituric-cinchonidine cocrystal are shown in Figure 8, and the correlation between the energies of the important absorption bands is shown in Table 4. All of the strong 5-nitrobarbiturate vibrational modes were noted to undergo shifts in energy relative to the free acid, providing a further demonstration that the entire ring system of the acid is involved in the cocrystal formation. The energy of the quinuclidine mode was barely shifted in the spectrum of the cocrystal, while the vibrational mode of the quinoline moiety was noted to undergo a significant increase in energy. These findings indicate that the predominant interaction with 5-nitrobarbituric acid took place at the quinoline group and that the degree of interaction with the tertiary nitrogen of the quinuclidine group was minimal.

3.6. The 1:1 Quinine Cocrystal Formed with 5-Nitrobarbituric Acid.

The XRPD patterns obtained for 5-nitrobarbituric acid, quinine, and the nitrobarbiturate-quinine cocrystal product are shown in Figure 9. In this system, formation of the 1:1 stoichiometric reaction product is very evident in the nonequivalence of the powder patterns, especially when the quinine-free base used to form the cocrystal could only be obtained in a quasicrystalline form regardless of its initial processing. It is interesting to note that even though

TABLE 4: Assignments of the major bands in the fingerprint region of the Raman spectra of 5-nitrobarbituric acid, cinchonidine, and their 1 : 1 cocrystal product.

| Assignment	Nitrobarbituric (cm^{-1})	Cocrystal (cm^{-1})	Cinchonidine (cm^{-1})	Assignment
Carbonyl in-plane bending mode	379	373		
Carbonyl out-of-plane bending mode	625	617		
Carbonyl out-of-plane bending mode	695	681		
N–H out-of-plane bending mode	846	843		
C–N stretching mode	1150	1132		
C–N deformation mode	1255	1252		
		1358	1359	Nonprotonated quinuclidine mode
		1591	1564	Nonprotonated quinoline mode
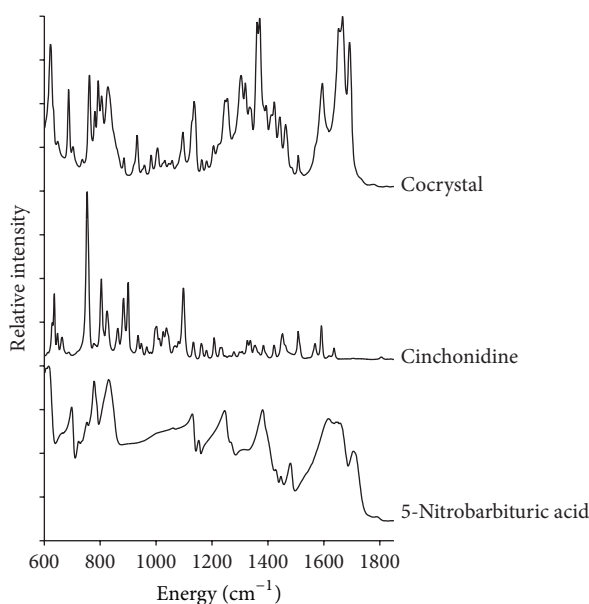
FIGURE 6: X-ray powder diffraction patterns of 5-nitrobarbituric acid, cinchonidine, and the 1 : 1 nitrobarbituric-cinchonidine cocrystal.

FIGURE 7: Infrared absorption spectra within the fingerprint region of 5-nitrobarbituric acid, cinchonidine, and the 1 : 1 nitrobarbituric-cinchonidine cocrystal.

the absolute configurations at the dissymmetric carbons of quinine and cinchonidine are the same, the XRPD patterns of their cocrystal products with 5-nitrobarbituric are only qualitatively similar and each exhibits peaks not contained in the pattern of the other.

However, like the nitrobarbiturate-cinchonidine cocrystal, the nitrobarbiturate-quinine cocrystal product was also found to be a 1.5-hydrate form, since it evolved 5.2% of its mass when heated isothermally at 125°C. The DSC thermogram of the nitrobarbiturate-quinine cocrystal product consisted of a strong desolvation endothermic transition, characterized by a temperature maximum of 98°C and an enthalpy of fusion equal to 74 J/g. The thermal characteristics of this desolvation endotherm are fairly similar to those of the nitrobarbiturate-cinchonidine cocrystal. Also akin to its stereochemical equivalent, the desolvated nitrobarbiturate-quinine cocrystal formed after completion of the desolvation thermal reaction exhibited a melting endothermic transition (temperature maximum of 217°C) that was accompanied by a strong exothermic decomposition reaction.
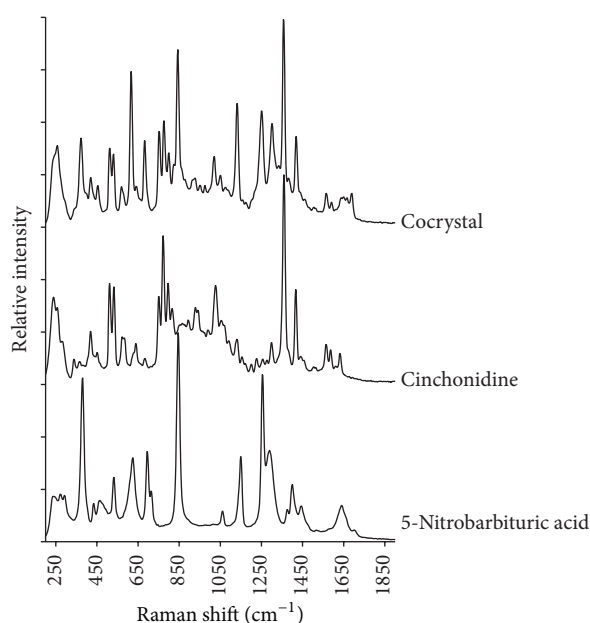
The fingerprint region infrared absorption spectra obtained for 5-nitrobarbituric acid, quinine, and the cocrystal product are shown in Figures 10 and 11, and the correlation between the energies of the important absorption bands is shown in Table 5. While the strong nitrobarbiturate absorption bands in the spectrum of the cocrystal were shifted in energy relative to the free acid, the pattern of shifting was somewhat different for the quinine cocrystal. For example, the energy of the carbonyl out-of-plane bending mode increased upon formation of the cocrystal, whereas in the two preceding systems the energy of this vibrational mode decreased.

Even more interesting was the behavior of the two key absorption bands of the quinuclidine and quinoline moieties of quinine. While these were obscured by the nitrobarbiturate absorption bands in the infrared absorption spectra of the cinchonine and cinchonidine cocrystal products, they were observed in the spectrum of the quinine cocrystal. However,

TABLE 5: Assignments of the major bands in the fingerprint region of the infrared absorption spectra of 5-nitrobarbituric acid, quinine, and their 1:1 cocrystal product.

| Assignment	Nitrobarbituric (cm^{-1})	Cocrystal (cm^{-1})	Quinine (cm^{-1})	Assignment
Carbonyl out-of-plane bending mode	779	791		
C–N ring deformation mode	1246	1234		
		1364	1371	Nonprotonated quinuclidine mode
Nitro group symmetric stretching mode	1381	1359		
		1575	1576	Nonprotonated quinoline mode
2-CO stretching mode	1614	1620		
4,6-CO antisymmetric mode	1651	1661		
4,6-CO symmetric mode	1705	1691		
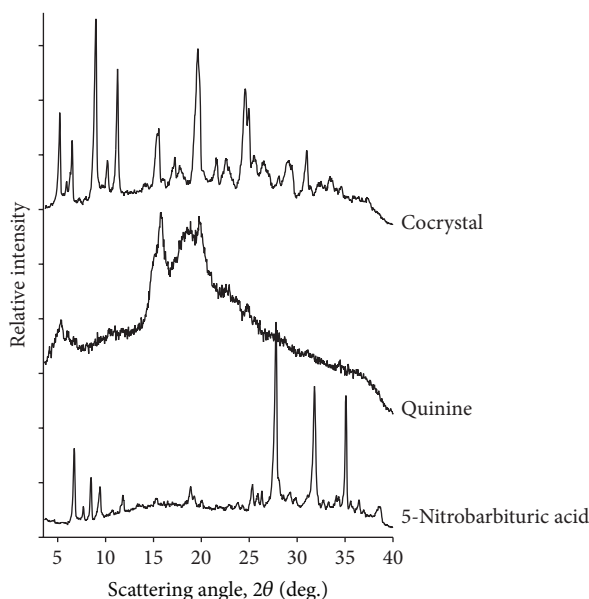
FIGURE 8: Raman spectra within the fingerprint region of 5-nitrobarbituric acid, cinchonidine, and the 1:1 nitrobarbituric-cinchonidine cocrystal.

FIGURE 9: X-ray powder diffraction patterns of 5-nitrobarbituric acid, quinine, and the 1:1 nitrobarbituric-quinine cocrystal.

the energy of the nonprotonated quinoline vibrational mode was only barely shifted in the spectrum of the cocrystal (1576 cm^{-1} for quinine versus 1575 cm^{-1} for its cocrystal), while the energy of the nonprotonated quinuclidine vibrational mode was definitely shifted (1371 cm^{-1} for quinine versus 1364 cm^{-1} for its cocrystal). This finding would imply that while the dominant interaction between 5-nitrobarbituric acid and cinchonine or cinchonidine was between the acid and the quinoline ring, the dominant interaction between 5-nitrobarbituric acid and quinine was between the acid and the quinuclidine ring nitrogen.

Quinine also contains a methoxy group bound on the quinoline ring that is not present for either cinchonine or cinchonidine. In the spectrum of the free base, the vibrational bands associated with the methoxy group were observed as a strong doublet of peaks (having energies of 1227 and 1240 cm^{-1}) that each underwent significant shifting in the spectrum of the cocrystal (1234 and 1252 cm^{-1}). This
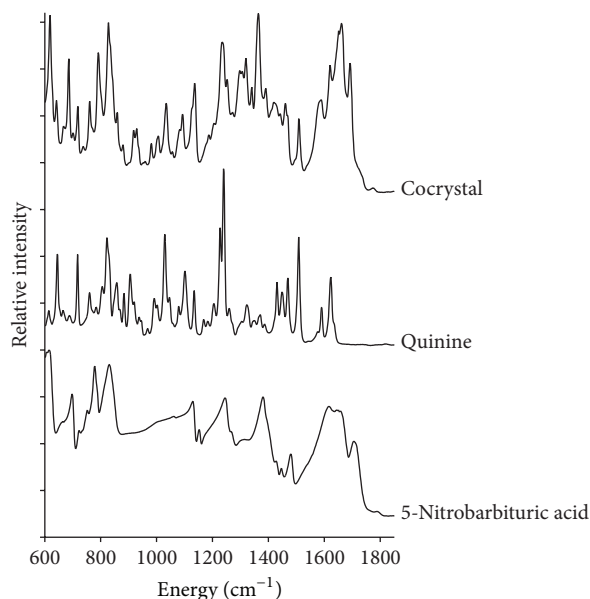
observation indicates that while the quinoline ring nitrogen was not strongly involved in the intermolecular interactions of the synthon, its methoxy group certainly was.

The fingerprint region Raman spectra obtained for 5-nitrobarbituric acid, quinine, and the 1:1 nitrobarbituric-quinine cocrystal are shown in Figure 10, and the correlation between the energies of the important absorption bands is shown in Table 6. The strong 5-nitrobarbiturate vibrational modes were found to undergo shifts in energy relative to the free acid, as would be expected since the entire ring system of the 5-nitrobarbituric acid is involved in the cocrystal formation. As had been noted in the infrared absorption spectra, the energy of the nonprotonated quinuclidine mode was significantly shifted in the spectrum of the cocrystal, while the vibrational mode of the nonprotonated quinoline group barely underwent any change in energy. These findings provide further support that the predominant interaction with 5-nitrobarbituric acid took place at the quinuclidine group.

TABLE 6: Assignments of the major bands in the fingerprint region of the Raman spectra of 5-nitrobarbituric acid, quinine, and their 1:1 cocrystal product.

| Assignment	Nitrobarbituric (cm^{-1})	Cocrystal (cm^{-1})	Quinine (cm^{-1})	Assignment
Carbonyl in-plane bending mode	379	368		
Carbonyl out-of-plane bending mode	625	610		
Carbonyl out-of-plane bending mode	695	679		
N–H out-of-plane bending mode	846	834		
C–N stretching mode	1150	1125		
C–N deformation mode	1255	1242		
		1359	1366	Nonprotonated quinuclidine mode
		1586	1585	Nonprotonated quinoline mode
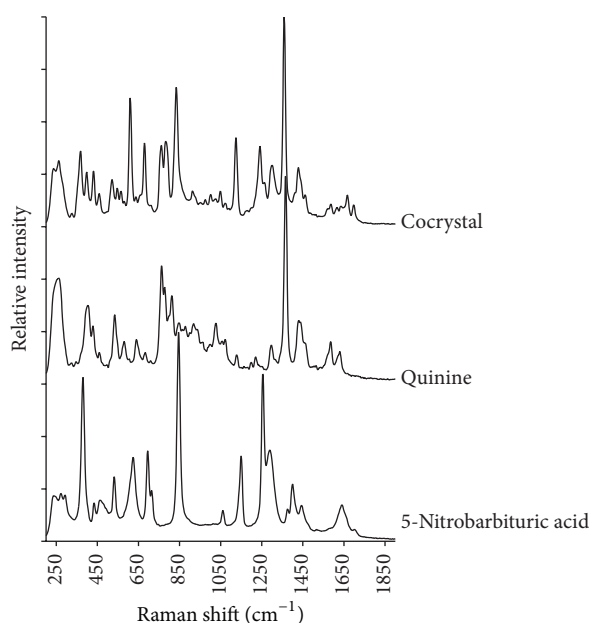
FIGURE 10: Infrared absorption spectra within the fingerprint region of 5-nitrobarbituric acid, quinine, and the 1:1 nitrobarbituric-quinine cocrystal.

FIGURE 11: Raman spectra within the fingerprint region of 5-nitrobarbituric acid, quinine, and the 1:1 nitrobarbituric-quinine cocrystal.

3.7. The 1:1 Quinidine Cocrystal Formed with 5-Nitrobarbituric Acid.

The XRPD patterns obtained for 5-nitrobarbituric acid, quinidine, and the nitrobarbiturate-quinidine cocrystal product are shown in Figure 12, where it may be noted that the degree of crystallinity associated with the cocrystal was substantially less than that of the reactants. Nevertheless, the unique diffraction pattern obtained for the 1:1 stoichiometric reaction pattern relative to those of the reactants establishes the existence of a genuine cocrystal.

The nitrobarbiturate-quinidine cocrystal product proved to be unique in that it barely evolved 0.25% of its mass when heated isothermally at 125°C and was therefore determined to be a nonsolvated solid-state form. This type of cocrystal product is totally different from that of its stereochemical analogue, as the nitrobarbiturate-cinchonine cocrystal product was characterized by the highest degree of hydration among the cocrystals studied. The DSC thermogram of the nitrobarbiturate-quinidine cocrystal product did not contain a desolvati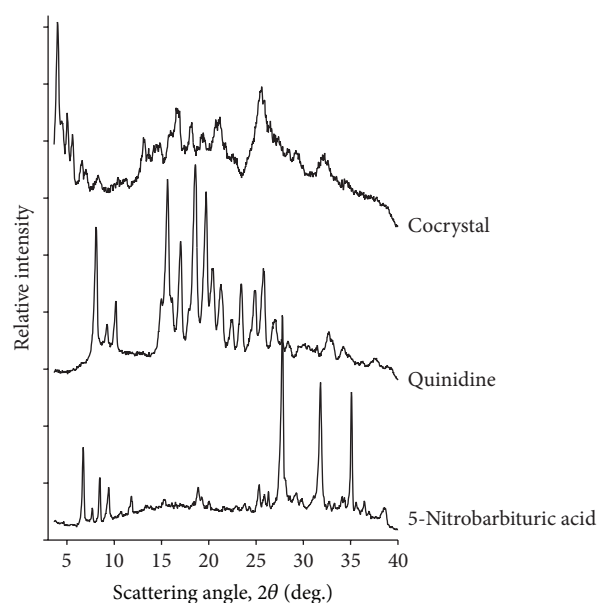on endotherm and instead consisted of a weak melting endothermic transition having a temperature maximum of 196°C and an enthalpy of fusion equal to 15 J/g. At a temperature of 230°C the cocrystal was found to undergo a strong exothermic decomposition reaction.

The fingerprint region infrared absorption spectra obtained for 5-nitrobarbituric acid, quinidine, and the cocrystal product are shown in Figure 13, and the correlation between the energies of the important absorption bands is shown in Table 7. The trends in vibrational energies of the strong nitrobarbiturate absorption bands in the spectrum of the cocrystal were found to be consistent with those of the cocrystals with cinchonine and cinchonidine, and the two key absorption bands of the quinuclidine and quinoline moieties of quinidine were obscured by the nitrobarbiturate absorption bands.

The fingerprint region Raman spectra obtained for 5-nitrobarbituric acid, quinidine, and the 1:1 nitrobarbituric-quinidine cocrystal are shown in Figure 14, and the correlation between the energies of the important absorption

TABLE 7: Assignments of the major bands in the fingerprint region of the infrared absorption spectra of 5-nitrobarbituric acid, quinidine, and their 1:1 cocrystal product.

Assignment	Nitrobarbituric (cm^{-1})	Cocrystal (cm^{-1})	Quinidine (cm^{-1})	Assignment
Carbonyl out-of-plane bending mode	779	756		
C–N ring deformation mode	1246	1240		
		Obscured and not observed	1360	Nonprotonated quinuclidine mode
Nitro group symmetric stretching mode	1381	1362		
		Obscured and not observed	1562	Nonprotonated quinoline mode
2-CO stretching mode	1614	1622		
4,6-CO antisymmetric mode	1651	Not observed		
4,6-CO symmetric mode	1705	1690		

TABLE 8: Assignments of the major bands in the fingerprint region of the Raman spectra of 5-nitrobarbituric acid, quinidine, and their 1:1 cocrystal product.

| Assignment	Nitrobarbituric (cm^{-1})	Cocrystal (cm^{-1})	Quinidine (cm^{-1})	Assignment
Carbonyl in-plane bending mode	379	365		
Carbonyl out-of-plane bending mode	625	608		
Carbonyl out-of-plane bending mode	695	681		
N–H out-of-plane bending mode	846	836		
C–N stretching mode	1150	1144		
C–N deformation mode	1255	1243		
		1362	1363	Nonprotonated quinuclidine mode
		1570	1561	Nonprotonated quinoline mode
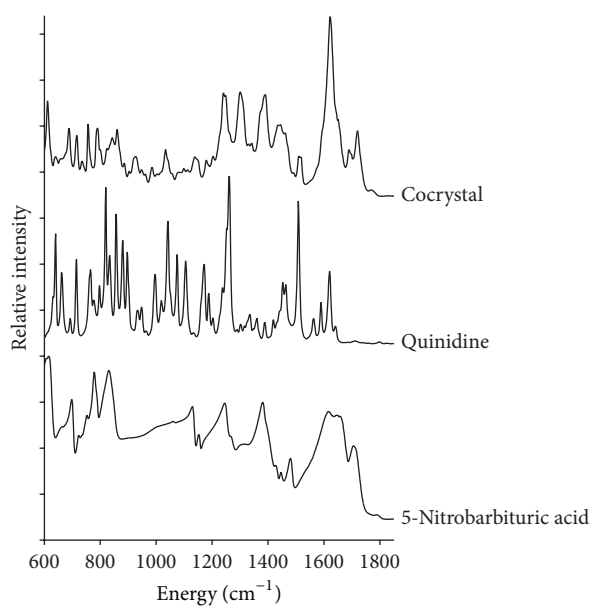
FIGURE 12: X-ray powder diffraction patterns of 5-nitrobarbituric acid, quinidine, and the 1:1 nitrobarbituric-quinidine cocrystal.

bands is shown in Table 8. All of the strong 5-nitrobarbiturate vibrational modes were noted to undergo shifts in energy relative to the free acid, confirming as before that the entire ring system of the acid is involved in the cocrystal formation. The energy of the nonprotonated quinuclidine mode (1363 cm^{-1}) was barely shifted in the spectrum of the cocrystal (1362 cm^{-1}), while the vibrational mode of the quinoline moiety was noted to undergo a significant increase in energy from 1561 cm^{-1} to 1570 cm^{-1}. These findings indicate that, in this cocrystal system, the predominant interaction with 5-nitrobarbituric acid took place at the quinoline group and that the degree of interaction with the tertiary nitrogen of the quinuclidine group was minimal.

4. Conclusions

X-ray powder diffraction and thermal analysis have been used to demonstrate the existence of new solid-state forms generated by the cocrystallization of 5-nitrobarbituric acid with four cinchona alkaloids. The cocrystal products were found to contain varying degrees of hydration, ranging from no hydration in the nitrobarbiturate-quinidine cocrystal up to a 4.5-hydrate species in the nitrobarbiturate-cinchonine cocrystal. Raman spectra of the products were used to determine the predominant mode of interaction in the nitrobarbiturate-cinchona synthon. For the nitrobarbiturate cocrystals with cinchonine, cinchonidine, and quinidine,
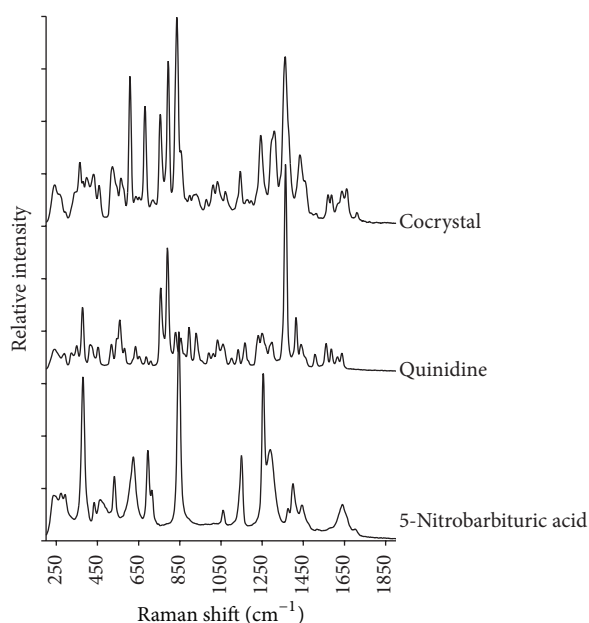
Figure 13: Infrared absorption spectra within the fingerprint region of 5-nitrobarbituric acid, quinidine, and the 1:1 nitrobarbituric-quinidine cocrystal.
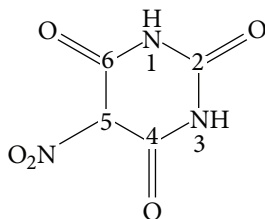

Figure 14: Raman spectra within the fingerprint region of 5-nitrobarbituric acid, quinidine, and the 1:1 nitrobarbituric-quinidine cocrystal.

the predominant interaction was with the quinoline ring system of the alkaloid. However, for quinine, the predominant interaction was with the quinuclidine group of the alkaloid.

Previous papers in this series [26, 27] have established that the variety of morphologies encountered for the molecular complexes of basic substances with 5-nitrobarbituric acid (dilituric acid) arises from the ability of the nitrobarbiturate reagent to form differing structural types and/or hydrates upon crystallization. The nonequivalence observed for the powder X-ray diffraction patterns demonstrates that each isolated adduct exhibits a unique crystal structure, which in turn yields differing crystal morphologies. This behavior has been further verified in the present study, where the differing range of hydrate and structural types would serve to easily differentiate the cinchona alkaloids from each other, even when different compounds contained the same absolute configurations at their dissymmetric centers.

Conflict of Interests

The author declares that there is no conflict of interests regarding the publication of this paper.

References

[1] P. Vishweshwar, J. A. McMahon, J. A. Bis, and M. J. Zaworotko, "Pharmaceutical co-crystals," *Journal of Pharmaceutical Sciences*, vol. 95, no. 3, pp. 499–516, 2006.

[2] N. Blagden, M. de Matas, P. T. Gavan, and P. York, "Crystal engineering of active pharmaceutical ingredients to improve solubility and dissolution rates," *Advanced Drug Delivery Reviews*, vol. 59, no. 7, pp. 617–630, 2007.

[3] N. Schultheiss and A. Newman, "Pharmaceutical cocrystals and their physicochemical properties," *Crystal Growth and Design*, vol. 9, no. 6, pp. 2950–2967, 2009.

[4] T. Friscic and W. Jones, *Journal of Pharmacology and Pharmacotherapeutics*, vol. 5, pp. 1547–1559, 2010.

[5] H. G. Brittain, "Pharmaceutical cocrystals: the coming wave of new drug substances," *Journal of Pharmaceutical Sciences*, vol. 102, no. 2, pp. 311–317, 2013.

[6] C. B. Aakeröy and D. J. Salmon, "Building co-crystals with molecular sense and supramolecular sensibility," *CrystEngComm*, vol. 7, pp. 439–448, 2005.

[7] A. I. Kitaigorodsky, *Mixed Crystals*, Springer, Berlin, Germany, 1984.

[8] F. H. Herbstein, *Crystalline Molecular Complexes and Compounds*, vol. 2, Oxford University Press, Oxford, UK, 2005.

[9] G. P. Stahly, "A survey of cocrystals reported prior to 2000," *Crystal Growth and Design*, vol. 9, no. 10, pp. 4212–4229, 2009.

[10] H. G. Brittain, "Cocrystal systems of pharmaceutical interest: 2010," *Crystal Growth and Design*, vol. 12, no. 2, pp. 1046–1054, 2012.

[11] H. G. Brittain, "Cocrystal systems of pharmaceutical interest: 2011," *Crystal Growth and Design*, vol. 12, no. 11, pp. 5823–5832, 2012.

[12] E. M. Chamot and C. W. Mason, *Handbook of Chemical Microscopy*, vol. 2, John Wiley & Sons, New York, NY, USA, 2nd edition, 1940.

[13] R. E. Stevens, "Organic chemical microscopy: a monograph," *Microchemical Journal*, vol. 13, no. 1, pp. 42–65, 1968.

[14] E. G. C. Clarke, "Microchemical identification of local anæsthetic drugs," *Journal of Pharmacy and Pharmacology*, vol. 8, no. 1, pp. 202–206, 1956.

[15] E. G. C. Clarke, "Microchemical identification of some antihistamine drugs," *Journal of Pharmacy and Pharmacology*, vol. 9, no. 11, pp. 752–758, 1957.

[16] E. G. C. Clarke, "A note on the identification of some antimalarial drugs," *Journal of Pharmacy and Pharmacology*, vol. 10, no. 1, pp. 194–196, 1958.

[17] E. G. C. Clarke, "Microchemical differentiation between optical isomers of *N*-methylmorphinan analgesics," *Journal of Pharmacy and Pharmacology*, vol. 10, pp. 642–644, 1958.

[18] N. W. Rich and L. G. Chatten, "Identification and differentiation of organic medicinal agents. I. Local anesthetics," *Journal of Pharmaceutical Sciences*, vol. 54, no. 7, pp. 995–1002, 1965.

[19] L. A. Doan and L. G. Chatten, "Identification and differentiation of organic medicinal agents II. Muscle relaxants," *Journal of Pharmaceutical Sciences*, vol. 54, no. 11, pp. 1605–1609, 1965.

[20] L. G. Chatten and L. A. Doan, "Identification and differentiation of organic medicinal agents. 3. Amine-containing antiparkinson agents and newer muscle relaxants," *Journal of Pharmaceutical Sciences*, vol. 55, no. 4, pp. 372–376, 1966.

[21] C. E. Redemann and C. Niemann, "The diliturates (5-nitrobarbiturates) of some physiologically important bases," *Journal of the American Chemical Society*, vol. 62, no. 3, pp. 590–593, 1940.

[22] E. M. Plein and B. T. Dewey, "Identification of organic bases by means of optical properties of diliturates (nitrobarbiturates) aliphatic amines," *Industrial & Engineering Chemistry Analytical Edition*, vol. 15, no. 8, pp. 534–536, 1943.

[23] B. T. Dewey and E. M. Plein, "Identification of organic bases by means of optical properties of diliturates (nitrobarbiturates) primary aromatic amines," *Industrial & Engineering Chemistry Analytical Edition*, vol. 18, no. 8, pp. 515–520, 1946.

[24] E. M. Plein, "The identification of some autonomic drugs by means of the optical properties of the diliturates," *Journal of the American Pharmaceutical Association*, vol. 38, no. 10, pp. 535–537, 1949.

[25] B. T. Dewey and E. M. Plein, "Crystallographic data. Identification of organic bases by means of optical properties of diliturates (nitrobarbiturates)," *Analytical Chemistry*, vol. 27, no. 5, pp. 862–863, 1955.

[26] H. G. Brittain, "Foundations of chemical microscopy. 2. Derivatives of primary phenylalkylamines with 5-nitrobarbituric acid," *Journal of Pharmaceutical and Biomedical Analysis*, vol. 19, no. 6, pp. 865–875, 1999.

[27] H. G. Brittain and M. Rehman, "Foundations of chemical microscopy. 3. Derivatives of some chiral phenylalkylamines and phenylalkylamino acids with 5-nitrobarbituric acid," *Chirality*, vol. 17, no. 2, pp. 89–98, 2005.

[28] E. T. Wherry and E. Yanovsky, "The identification of the cinchona alkaloids by optical-crystallographic measurements," *Journal of the American Chemical Society*, vol. 40, no. 7, pp. 1063–1074, 1918.

[29] B. E. Nelson and H. A. Leonard, "Identification of alkaloids under the microscope from the form of their picrate crystals," *Journal of the American Chemical Society*, vol. 44, no. 2, pp. 369–373, 1922.

[30] M. L. Shaner and M. L. Willard, "Optical crystallographic data for some salts of the cinchona alkaloids," *Journal of the American Chemical Society*, vol. 58, no. 10, pp. 1977–1978, 1936.

[31] V. R. Pedireddi, W. Jones, A. P. Chorlton, and R. Docherty, "Creation of crystalline supramolecular arrays: a comparison of co-crystal formation from solution and by solid-state grinding," *Chemical Communications*, no. 8, pp. 987–988, 1996.

[32] N. Shan, F. Toda, and W. Jones, "Mechanochemistry and co-crystal formation: effect of solvent on reaction kinetics," *Chemical Communications*, no. 20, pp. 2372–2373, 2002.

[33] A. V. Trask and W. Jones, "Crystal engineering of organic cocrystals by the solid-state grinding approach," in *Organic Solid State Reactions*, vol. 254 of *Topics in Current Chemistry*, pp. 41–70, Springer, Berlin, Germany, 2005.

[34] G. G. Lyle and L. K. Keefer, "The configurations at C-9 of the cinchona alkaloids. NMR spectral study of the derived oxiranes," *Tetrahedron*, vol. 23, no. 8, pp. 3253–3263, 1967.

[35] H. G. Brittain, "Circularly polarized luminescence studies of the optical activity induced in the europium(III) chelate of 4,4,4-trifluoro-1-(2-thienyl)butane-1,3-dionate through adduct formation with cinchona alkaloids," *Journal of the Chemical Society, Dalton Transactions*, vol. 1980, pp. 2369–2373, 1980.

[36] W. Klyne and J. Buckingham, *Atlas of Stereochemistry*, vol. 1, Oxford University Press, New York, NY, USA, 1974.

[37] O. L. Carter, A. T. McPhail, and G. A. Sim, "Optically active organometallic compounds. Part I. Absolute configuration of (-)-1,1'-dimethylferrocene-3-carboxylic acid by X-ray analysis of its quinidine salt," *Journal of the Chemical Society A: Inorganic, Physical, and Theoretical Chemistry*, pp. 365–373, 1967.

[38] J. T. Bojarski, J. L. Mokrosz, H. J. Bartoń, and M. H. Paluchowska, "Recent progress in barbituric acid chemistry," *Advances in Heterocyclic Chemistry*, vol. 38, pp. 229–297, 1985.

[39] W. C. Price, J. E. S. Bradley, and R. D. B. Fraser, "The relationship between the infra-red absorption spectra of some 5:5′-substituted barbituric acids and their pharmacological activity," *The Journal of Pharmacy and Pharmacology*, vol. 6, no. 8, pp. 522–528, 1954.

[40] S. Pinchas, "Charge transfer interaction between 2,3 dichloro 5,6 dicyano p-benzoquinone and aromatic hydrocarbons," *Spectrochimica Acta*, vol. 22, no. 11, pp. 1869–1895, 1966.

[41] R. J. Mesley, "Spectra-structure correlations in polymorphic solids—II. 5,5-Disubstituted barbituric acids," *Spectrochimica Acta Part A: Molecular Spectroscopy*, vol. 26, no. 7, pp. 1427–1448, 1970.

[42] A. J. Barnes, L. Le Gall, and J. Lauransan, "Vibrational spectra of barbituric acid derivatives in low-temperature matrices: part 2. Barbituric acid and 1,3-dimethyl barbituric acid," *Journal of Molecular Structure*, vol. 56, pp. 15–27, 1979.

[43] N. B. Colthup, L. H. Daly, and S. E. Wiberley, *Introduction to Infrared and Raman Spectroscopy*, Academic Press, New York, NY, USA, 1964.

[44] R. T. Conley, *Infrared Spectroscopy*, Allyn and Bacon, Boston, Mass, USA, 1966.

[45] F. F. Bentley, L. D. Smithson, and A. L. Rozel, *Infrared Spectra and Characteristic Frequencies 700-300 cm^{-1}*, Interscience, New York, NY, USA, 1968.

[46] L. J. Bellamy, *Advances in Infrared Group Frequencies*, Methuen & Co, London, UK, 1968.

[47] F. R. Dollish, W. G. Fateley, and F. F. Bentley, *Characteristic Raman Frequencies of Organic Compounds*, John Wiley & Sons, New York, NY, USA, 1974.

[48] J. G. Grasselli, M. K. Snavely, and B. J. Bulkin, *Chemical Applications of Raman Spectroscopy*, John Wiley & Sons, New York, NY, USA, 1981.

[49] G. Socrates, *Infrared and Raman Characteristic Group Frequencies*, John Wiley & Sons, Chichester, UK, 3rd edition, 2001.

[50] I. R. Lewis and H. G. M. Edwards, *Handbook of Raman Spectroscopy*, Marcel Dekker, New York, NY, USA, 2001.

[51] S. C. Wait Jr. and J. C. McNerney, "Vibrational spectra and assignments for quinoline and isoquinoline," *Journal of Molecular Spectroscopy*, vol. 34, no. 1, pp. 56–77, 1970.

[52] A. E. Özel, Y. Büyükmurat, and S. Akyüz, "Infrared-spectra and normal-coordinate analysis of quinoline and quinoline complexes," *Journal of Molecular Structure*, vol. 565-566, pp. 455–462, 2001.

[53] P. Bruesch, "X-ray and infrared studies of bicyclo(2.2.2) octane, triethylenediamine and quinuclidine—II. Normal co-ordinate calculations of bicyclo(2.2.2.)octane, triethylenediamine and quinuclidine," *Spectrochimica Acta*, vol. 22, no. 5, pp. 867–875, 1966.

[54] P. Bruesch and H. H. Gunthard, "X-ray and infra-red studies of bicyclo(2.2.2)octane, triethylenediamine and quinuclidine—III. Assignments of high and low temperature infra-red spectra.

Comparison with X-ray results," *Spectrochim Acta*, vol. 22, no. 5, pp. 877–887, 1966.

[55] A. Weselucha-Birczyńska and M. Ciechanowicz-Rutkowska, "Experimental and calculated structure of vibrational spectra of cinchonine," *Journal of Molecular Structure*, vol. 555, pp. 391–395, 2000.

[56] W. Chu, R. J. LeBlanc, and C. T. Williams, "In-situ Raman investigation of cinchonidine adsorption on polycrystalline platinum in ethanol," *Catalysis Communications*, vol. 3, no. 12, pp. 547–552, 2002.

[57] T. Frosch, M. Schmtt, and J. Popp, "In situ UV resonance Raman micro-spectroscopic localization of the antimalarial quinine in cinchona bark," *Journal of Physical Chemistry B*, vol. 111, no. 16, pp. 4171–4177, 2007.

International Journal of
Medicinal Chemistry

Organic Chemistry
International

International Journal of
Photoenergy

International Journal of
Analytical Chemistry

Advances in
Physical Chemistry

International Journal of
Carbohydrate
Chemistry

Journal of
Quantum Chemistry

The Scientific
World Journal

Submit your manuscripts at
http://www.hindawi.com

Hindawi

Journal of
Analytical Methods
in Chemistry

Journal of
Spectroscopy

International Journal of
Inorganic Chemistry

International Journal of
Electrochemistry

Journal of
Applied Chemistry

Bioinorganic Chemistry
and Applications

Journal of
Theoretical Chemistry

Chromatography
Research International

Journal of
Catalysts

Journal of
Chemistry

International Journal of
Spectroscopy